Electronic Supplementary Information

Charge Transfer Induced by Electronic State Mixing in a Symmetric X-Y-X-type Multi-Chromophore System

Siin Kim,[a,b] Doo-Sik Ahn,[a,b] Mina Ahn,[c] Kyung-Ryang Wee,[c] Jungkweon Choi[a,b]* and Hyotcherl Ihee[a,b]*

a. Department of Chemistry and KI for the BioCentury, Korea Advanced Institute of Science and Technology (KAIST), Daejeon 34141, Republic of Korea

b. Center for Nanomaterials and Chemical Reactions, Institute for Basic Science, Daejeon 34141, Republic of Korea

c. Department of Chemistry, Daegu University, Gyeongsan 38453, Republic of Korea

* Corresponding authors: Jungkweon Choi and Hyotcherl Ihee

E-mail: jkchoi@ibs.re.kr, hyotcherl.ihee@kaist.ac.kr

Experimental section

General. Based on standard Schlenk techniques, the synthesis experimental procedure was performed under a dry argon condition. Commercially available reagents and solvents were used without further purification. Reaction was monitored with thin layer chromatography (TLC) using commercial TLC plates (Merck Co.). Silica gel column chromatography was performed on silica gel 60 G (230–400 mesh ASTM, Merck Co.). The synthesized compound was characterized by ^{1}H-NMR or ^{13}C-NMR, and elemental analysis. The ^{1}H and proton-decoupled ^{13}C spectra were recorded on a Bruker500 spectrometer operating at 500 and 125 MHz, respectively, and all proton and carbon chemical shifts were measured relative to internal residual chloroform (99.5 % $CDCl_3$) or dimethyl sulfoxide (99.8 % DMSO-d_6) from the lock solvent. The elemental analysis (C, H) was performed using Thermo Fisher Scientific Flash 2000 series analyzer. The GC-MS analysis was performed using a highly sensitive Gas Chromatograph/Mass Selective Detector spectrometer (Agilent, 7890B-5977B GC/MSD).

Synthesis of 1-phenylpyrene. A mixture of bromobenzene (0.5 g, 3.18 mmol), pyrene-1-boronic acid (0.78 g, 3.18 mmol), $Pd(PPh_3)_4$ (0.02 g, 5 mol%), K_2CO_3 (1.32 g, 9.55 mmol) in Toluene/H_2O (*v*/*v* = 40 mL/10 mL) was refluxed under argon at 110 ℃ for overnight. After cooling to room temperature, deionized water (50 ml) was poured and organic layer was separated using a separating funnel. The water layer was washed using methylene chloride (×3) for extracted remained organic residue. After combined all of organic solvents, the organic layer was dried over anhydrous $MgSO_4$ and then filtered off. The solvent was removed under reduced pressure, and the resultant residue was purified by silica gel column chromatography (CH_2Cl_2/*n*-hexane 1:10) to afford Py-Benz as a white solid (0.45 g, 51 %); ^{1}H NMR (500 MHz, $CDCl_3$, ppm) δ 8.27-8.20 (m, 4H), 8.14 (s, 2H), 8.07-8.02 (m, 3H), 7.69 (d, J = 7.0 Hz, 2H), 7.61 (t, J = 7.0 Hz, 2H), 7.54 (t, J = 7.5 Hz, 1H). ^{1}H NMR (500 MHz, DMSO-d_6, ppm) δ 8.34-8.30 (dd, J = 11.5, 7.5 Hz, 2H), 8.25 (d, J = 7.5 Hz, 1H), 8.20 (s, 2H), 8.14-8.06 (m, 3H), 7.98 (d, J = 8.0 Hz, 1H), 7.62-7.58 (m, 4H), 7.54-7.50 (m, 1H). ^{13}C{^{1}H} (125 MHz, DMSO-d_6, ppm) δ 140.8, 137.6, 131.5, 130.9, 130.7, 130.6, 129.1, 128.2, 128.1, 127.9, 127.9, 127.8, 126.9, 125.8, 125.45, 125.38, 125.0, 124.6, 124.5. GC-MS Calcd for [$C_{22}H_{14}$]: 278.35 m/z, Found: 278.1 m/z. Elem. Anal. Found (Calcd) for $C_{22}H_{14}$: C, 94.98 (94.93); H, 5.02 (5.07).

Materials: Py-Benz-Py (> 98.0%) and bromobenzene (> 99.0 %) was purchased from TCI Co., Ltd and pyrene-1-boronic acid (Alfa-Aesar, > 95%), $Pd(PPh_3)_4$ (Sigma-Aldrich, > 99%), and K_2CO_3 (Alfa-Aesar, > 99%) were purchased from Alfa-Aesar and Sigma Aldrich. All reagents were used without further purification. All solvents (CHX: > 99.9%, Tol: > 99.5%, EE: > 99.7%, THF: > 99.9%, DCM: > 99.5%, and MeCN: > 99.5%,) were purchased from Sigma Aldrich, SAMCHUN, or TCI Co., Ltd and used without further purification.

Steady-state absorption and emission spectroscopy, and time-correlated single-photon counting. We used a UV-visible spectrophotometer (Shimadzu, UV-2550) and a fluorometer (PerkinElmer, LS-55) for the measurement of absorption and emission spectra, respectively. All sample solutions were placed into quartz cells with 1 cm width. The fluorescence lifetime was measured with a time-correlated single-photon counting (TCSPC) spectrometer (Edinburgh Instruments, FL920). The samples were excited with 375 nm pulses from a diode laser and the instrument response function of the TCSPC spectrometer was 270 ps.

The relative emission quantum yield was calculated using the following equation,

$$\Phi = \frac{F^s a_r n_s^2}{F^r a_s n_r^2} \Phi^r \quad (1)$$

where Φ and Φ^r represent the relative emission quantum yield of the sample and the reference sample, respectively. The subscripts s and r represent the sample and the reference, respectively. F corresponds to the integrated area of each emission band, and a is the absorbance, and n is the refractive index of the solvent.[1] Here, we used the quantum yield (Φ = 0.61) of Py-Benz-Py in dichloromethane reported by Kim et al.[2] To estimate the radiative and nonradiative decay constants, we used the following equations:

$$k_R = \Phi / \tau \quad (2)$$

$$k_{NR} = 1/\tau - k_R \quad (3)$$

where Φ is the emission quantum yield calculated by the eq 1 and τ is the emission lifetime obtained from TCSPC.

The relation between Stokes shifts and solvent polarity (Δf) is quantitatively analyzed with Lippert-Mataga equation (Figure S18, eq 4 and 5)

$$\Delta\tilde{\nu} = \tilde{\nu}\text{abs} - \tilde{\nu}\text{emi} = \frac{2\Delta\mu^2\Delta f}{hca_0^3} + \text{constant} \quad (4)$$

$$\Delta f = \frac{\varepsilon - 1}{2\varepsilon + 1} - \frac{n^2 - 1}{2n^2 + 1} \quad (5)$$

where $\tilde{\nu}\text{abs}$ and $\tilde{\nu}\text{emi}$ represent the wavenumber of absorption and emission maxima, $\Delta\mu$ is the difference between the dipole moments of excited state and the ground state, h is the Planck's constant, c is the speed of light, a_0 is the radius of the chromophore based on the Onsager's model, n is the refractive index of solvent, and ε is the dielectric constant of solvent.

Femtosecond transient absorption (TA) spectroscopy. The TA spectra were collected using a pump–probe transient absorption spectroscopy system. The pump light was generated using a regenerative amplified titanium sapphire laser system (Spectra-Physics, Spitfire Ace, 1 kHz) pumped by a diode-pumped Q-switched laser (Spectra-Physics, Empower). The seed pulse was generated using a titanium sapphire laser (Spectra-Physics, MaiTai SP). The pulses (350 nm) generated from an optical parametric amplifier (Spectra-Physics, OPAS prime) were used as the excitation beam. A white light continuum pulse, which was generated by focusing the residual of the fundamental light onto a 1 mm path length quartz cell containing water, was used as a probe beam. The white light was directed to the sample cell with an optical path of 2.0 mm and detected with a CCD detector installed in the absorption spectroscopy system after the controlled optical delay. The pump pulse was chopped by a mechanical chopper synchronized to one-half of the laser repetition rate, resulting in a pair of spectra with and without the pump, from which the absorption change induced by the pump pulse was estimated.

DFT and TDDFT calculations. Crawford et al. showed that the calculation results for Py using B3LYP and CAM-B3LYP functionals can well reproduce its experimental absorption spectrum in terms of the vertical excitation energy of each transition, indicating that B3LYP and CAM-B3LYP are good functionals for predicting the trend in vertical excitation energies of Py and its derivatives.[3] Contrary to the vertical excitation energy, the calculated oscillator strengths show the dependence on the used functional. For instance, the B3LYP functional shows the higher oscillator strength for the $S_0 \rightarrow S_1$ transition whereas CAM-B3LYP exhibits the higher oscillator strength for the $S_0 \rightarrow S_2$ transition. The latter is consistent with the

experimental result. We also used two functionals to calculate the electronic states of Py. The calculation results are listed in Table S1. When CAM-B3LYP is used for TDDFT calculation, the oscillator strengths for all transitions are well reproduced.

The molecular structures of Py-Benz-Py were obtained from DFT calculations using the B3LYP functional with 6-31G* basis sets. For the geometry optimizations in the S_1 state, TDDFT calculations were implemented. To unveil the excited-state character of the Py-Benz-Py, we implemented the time-dependent density functional theory (TDDFT) calculations with B3LYP and CAM-B3LYP levels of theory with 6-31G* and cc-pVTZ basis sets (Table S2 and Figure S7). All calculations were performed using the Gaussian 09 package.[4]

References

1. A. M. Brouwer, *Pure Appl. Chem.*, 2011, **83**, 2213-2228.
2. C. W. Kim, S. N. Park, S. B. Lee, J. J. Kim, H. W. Lee, Y. K. Kim and S. S. Yoon, *J. Nanosci. Nanotechnol.*, 2016, **16**, 2912-2915.
3. A. G. Crawford, A. D. Dwyer, Z. Liu, A. Steffen, A. Beeby, L.-O. Pålsson, D. J. Tozer and T. B. Marder, *J. Am. Chem. Soc.*, 2011, **133**, 13349-13362.
4. Gaussian 09, Revision A.02, M. J. Frisch, G. W. Trucks, H. B. Schlegel, G. E. Scuseria, M. A. Robb, J. R. Cheeseman, G. Scalmani, V. Barone, G. A. Petersson, H. Nakatsuji, X. Li, M. Caricato, A. Marenich, J. Bloino, B. G. Janesko, R. Gomperts, B. Mennucci, H. P. Hratchian, J. V. Ortiz, A. F. Izmaylov, J. L. Sonnenberg, D. Williams-Young, F. Ding, F. Lipparini, F. Egidi, J. Goings, B. Peng, A. Petrone, T. Henderson, D. Ranasinghe, V. G. Zakrzewski, J. Gao, N. Rega, G. Zheng, W. Liang, M. Hada, M. Ehara, K. Toyota, R. Fukuda, J. Hasegawa, M. Ishida, T. Nakajima, Y. Honda, O. Kitao, H. Nakai, T. Vreven, K. Throssell, J. A. Montgomery, Jr., J. E. Peralta, F. Ogliaro, M. Bearpark, J. J. Heyd, E. Brothers, K. N. Kudin, V. N. Staroverov, T. Keith, R. Kobayashi, J. Normand, K. Raghavachari, A. Rendell, J. C. Burant, S. S. Iyengar, J. Tomasi, M. Cossi, J. M. Millam, M. Klene, C. Adamo, R. Cammi, J. W. Ochterski, R. L. Martin, K. Morokuma, O. Farkas, J. B. Foresman, and D. J. Fox, Gaussian, Inc., Wallingford CT, 2016.

Table S1. Vertical excitation energies of Py calculated with various functionals and basis sets

Ground state	Vertical transition	State	λ_{ex} (nm)	Oscillator strength
B3LYP/6-31G*	B3LYP/cc-pVTZ	$S_0 \rightarrow S_1$	339.7	0.2507
		$S_0 \rightarrow S_2$	333.1	0.0003
B3LYP/6-31G*	CAM-B3LYP/cc-pVTZ	$S_0 \rightarrow S_1$	315.9	0.0003
		$S_0 \rightarrow S_2$	314.5	0.3101
CAM-B3LYP/6-31G*	CAM-B3LYP/cc-pVTZ	$S_0 \rightarrow S_1$	307.2	0.0001
		$S_0 \rightarrow S_2$	304.5	0.3106
B3LYP/cc-pVTZ	B3LYP/cc-pVTZ	$S_0 \rightarrow S_1$	336.6	0.2518
		$S_0 \rightarrow S_2$	329.9	0.0003
CAM-B3LYP/cc-pVTZ	CAM-B3LYP/cc-pVTZ	$S_0 \rightarrow S_1$	307.2	0.0004
		$S_0 \rightarrow S_2$	305.4	0.3052
B3LYP/6-31G*	B3LYP/6-31G*	$S_0 \rightarrow S_1$	333.1	0.2554
		$S_0 \rightarrow S_2$	327.5	0.0000

Table S2. Vertical excitation energies of Py-Benz-Py calculated with various functionals and basis sets

	Ground state	Vertical transition	State	λ_{ex} (nm)	Oscillator strength
1	B3LYP/6-31G*	B3LYP/cc-pVTZ	$S_0 \rightarrow S_1$	394.75	0.6951
			$S_0 \rightarrow S_2$	373.53	0.0004
2	B3LYP/6-31G*	CAM-B3LYP/cc-pVTZ	$S_0 \rightarrow S_1$	341.31	1.0912
			$S_0 \rightarrow S_2$	323.86	0.2295
3	CAM-B3LYP/6-31G*	CAM-B3LYP/cc-pVTZ	$S_0 \rightarrow S_1$	331.4	1.0329
			$S_0 \rightarrow S_2$	316.41	0.2168
4	B3LYP/cc-pVTZ	B3LYP/cc-pVTZ	$S_0 \rightarrow S_1$	388.53	0.6684
			$S_0 \rightarrow S_2$	368.61	0.0004
5	CAM-B3LYP/cc-pVTZ	CAM-B3LYP/cc-pVTZ	$S_0 \rightarrow S_1$	326.61	0.9814
			$S_0 \rightarrow S_2$	313.09	0.2221
6	B3LYP/6-31G*	B3LYP/6-31G*	$S_0 \rightarrow S_1$	389.09	0.6821
			$S_0 \rightarrow S_2$	369.7	0.0005

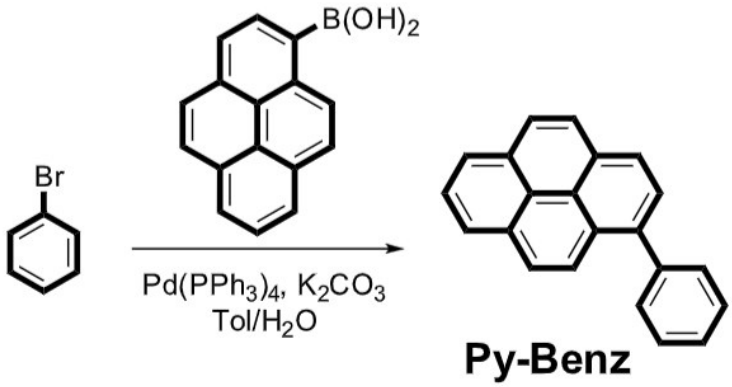

Figure S1. Synthesis route and molecular structure of Py-Benz.

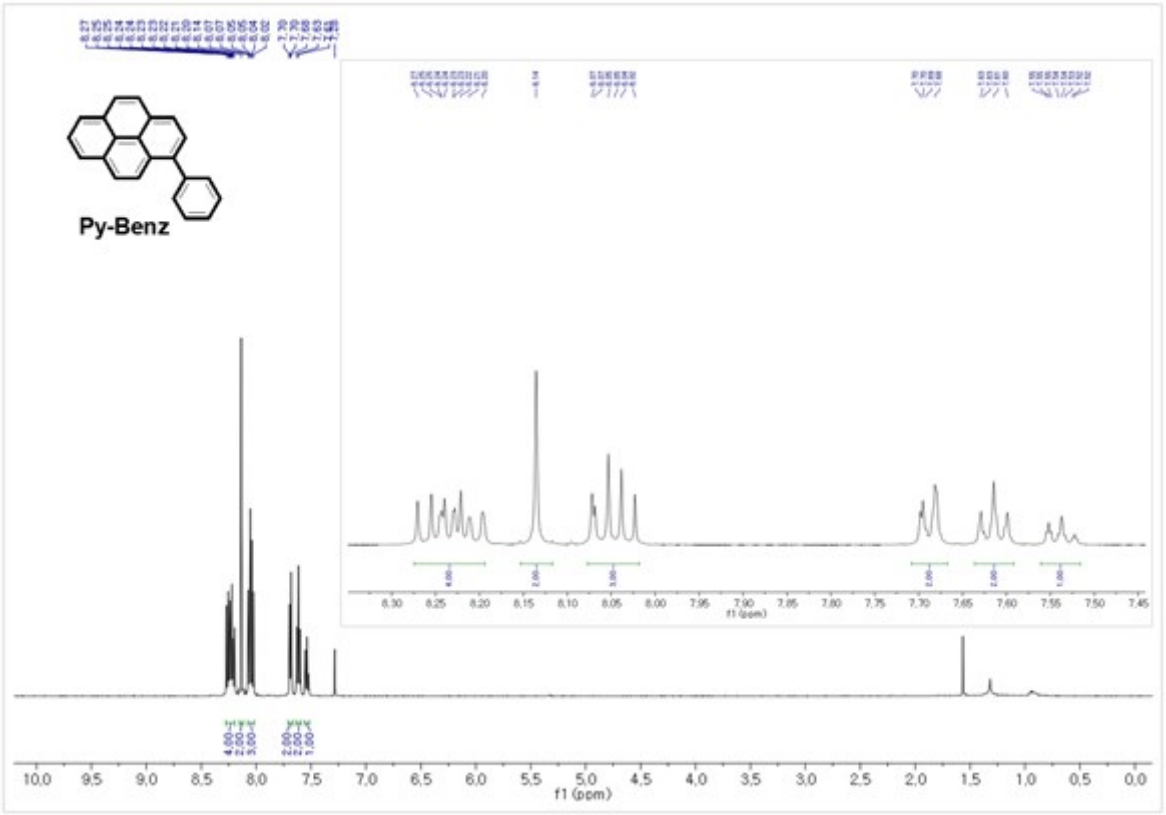

Figure S2. ^{1}H-NMR spectra of Py-Benz in $CDCl_3$ (500MHz, 293K).

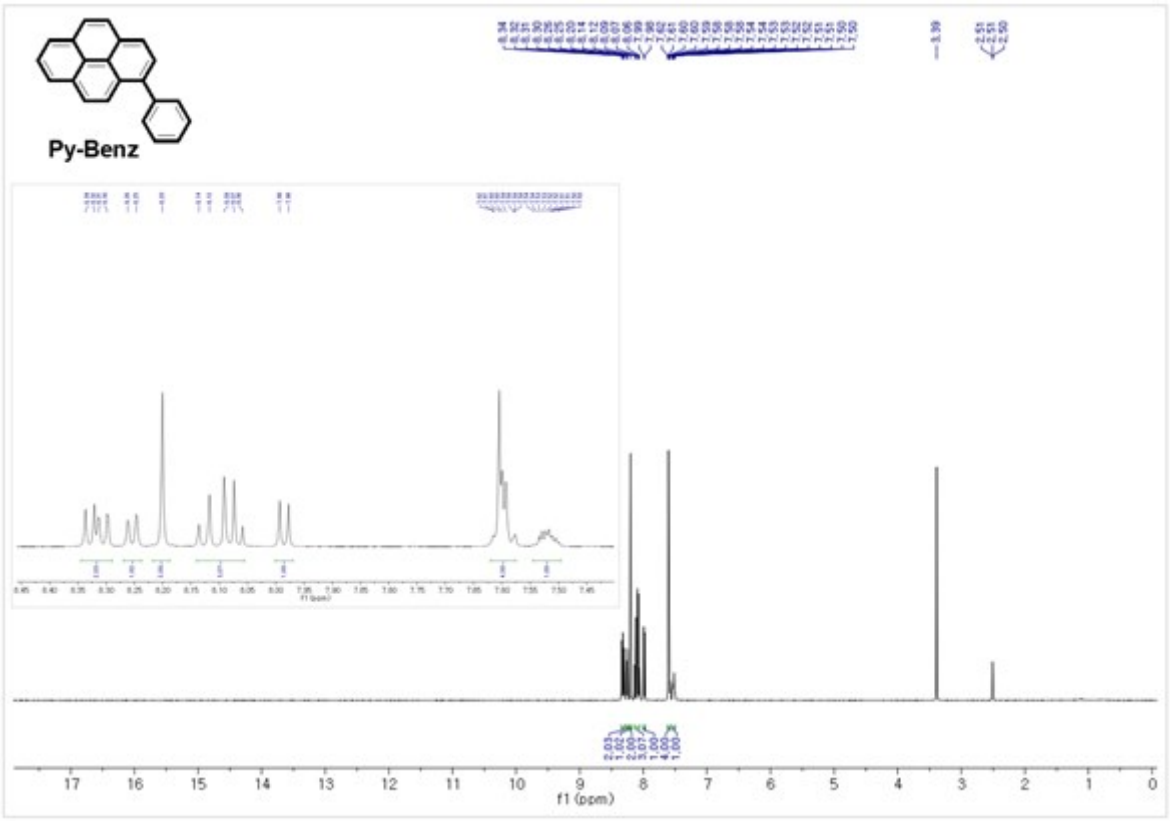

Figure S3. ^{1}H-NMR spectra of Py-Benz in DMSO-d_6 (500MHz, 293K).

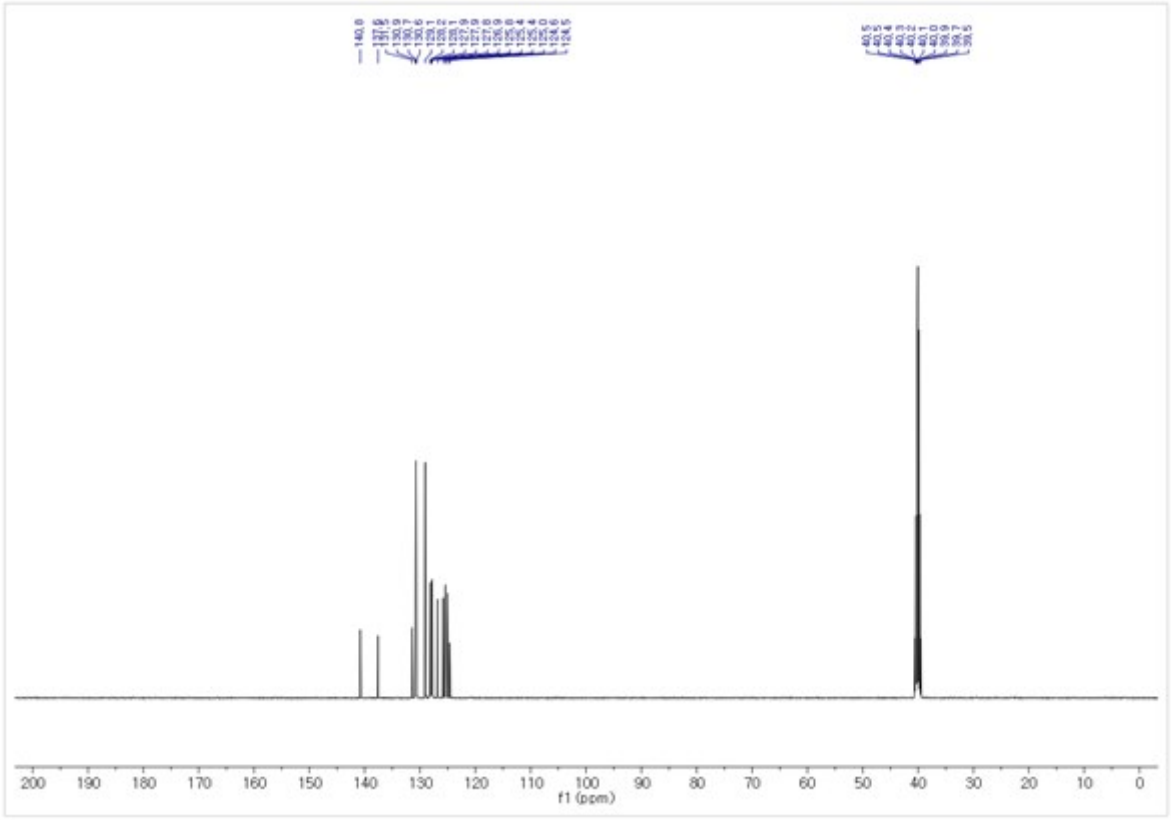

Figure S4. $^{13}C\{^{1}H\}$-NMR spectra of Py-Benz in DMSO-d_6 (125MHz, 293K).

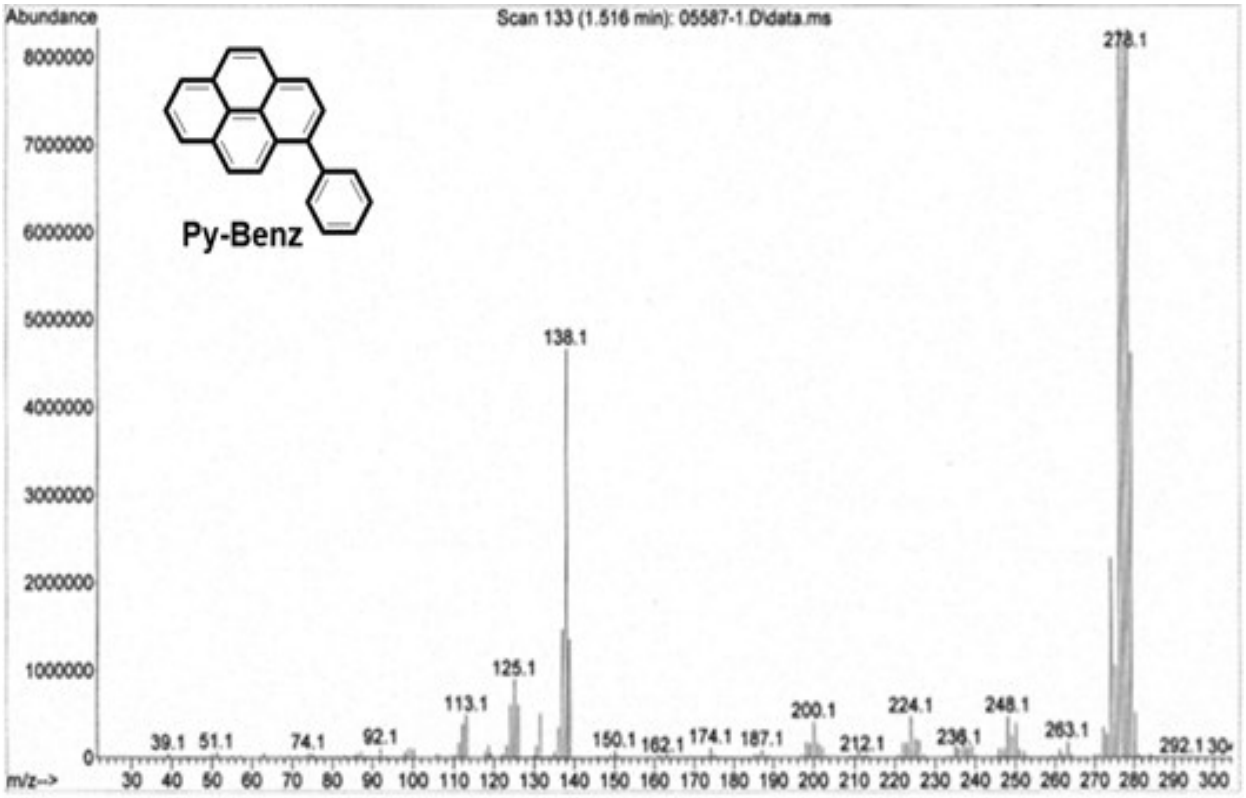

Figure S5. GC-MS data of Py-Benz.

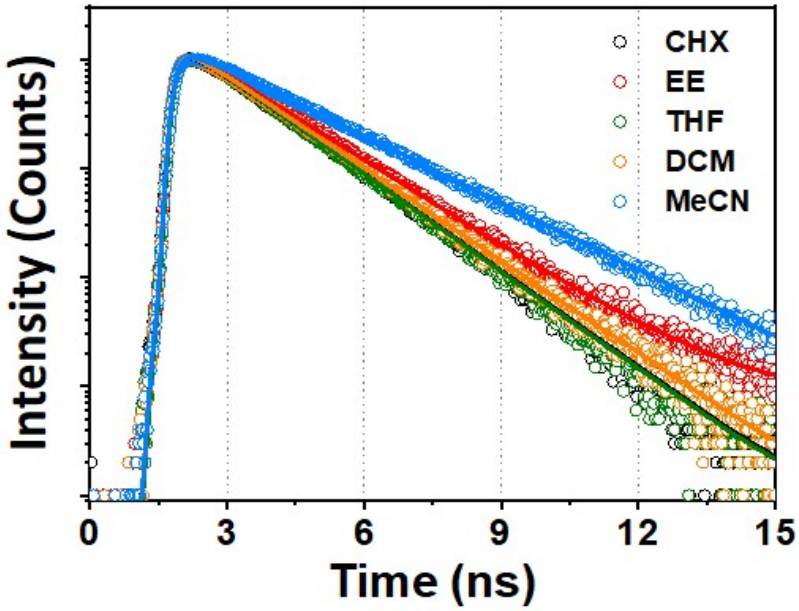

Figure S6. Time-correlated single-photon counting (TCSPC) data of Py-Benz-Py in CHX (black), EE (red), THF (green), DCM (orange), and MeCN (blue) and their fit. The excitation wavelength is 375 nm.

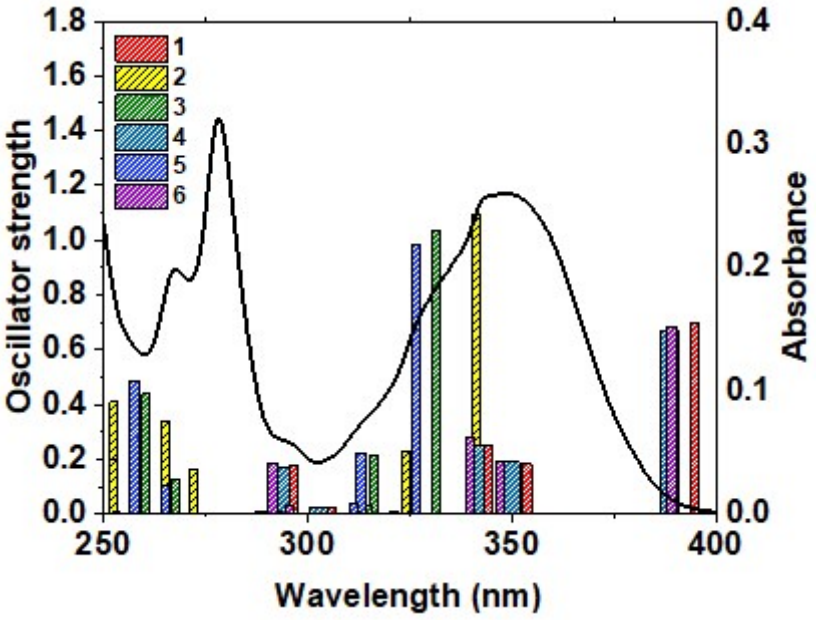

Figure S7. UV-visible absorption spectrum (black solid line) and the calculated oscillator strengths of Py-Benz-Py are depicted for all cases listed in Table S2. The B3LYP functional was used for 1, 4, and 6 to determine the vertical excitation energies. The CAM-B3LYP functional was used for 2,3, and 5 to determine the vertical excitation energies.

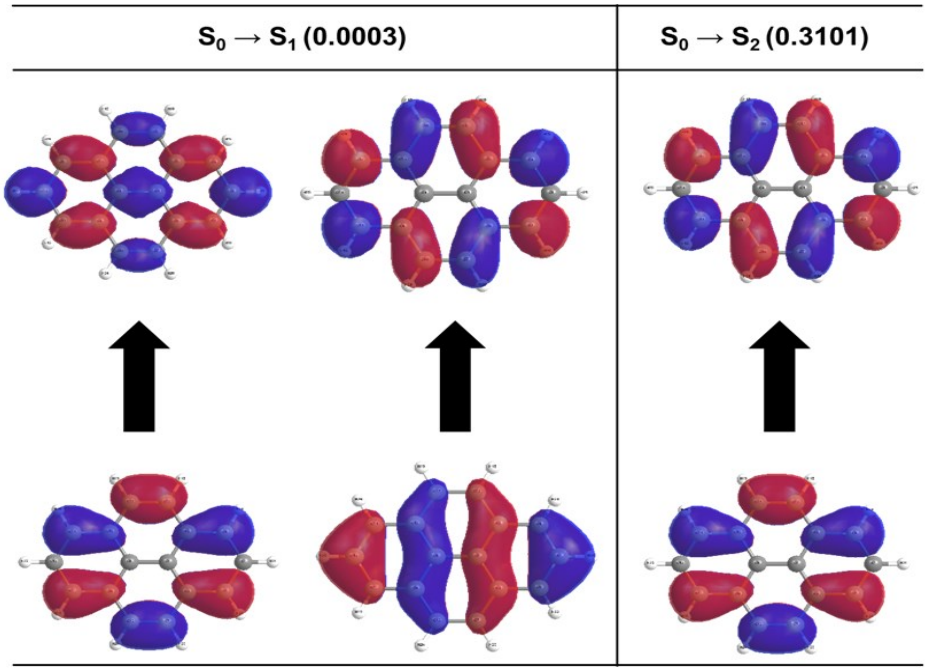

Figure S8. The molecular orbitals of two transitions ($S_0 \rightarrow S_1$ and $S_0 \rightarrow S_2$) of Py computed with TDDFT using CAM-B3LYP/cc-pVTZ. The oscillator strength of each transition is given in parentheses. Red and blue colors represent the different phases of the wavefunctions of molecular orbitals and the isovalue is 0.02 $e^-/Å^3$.

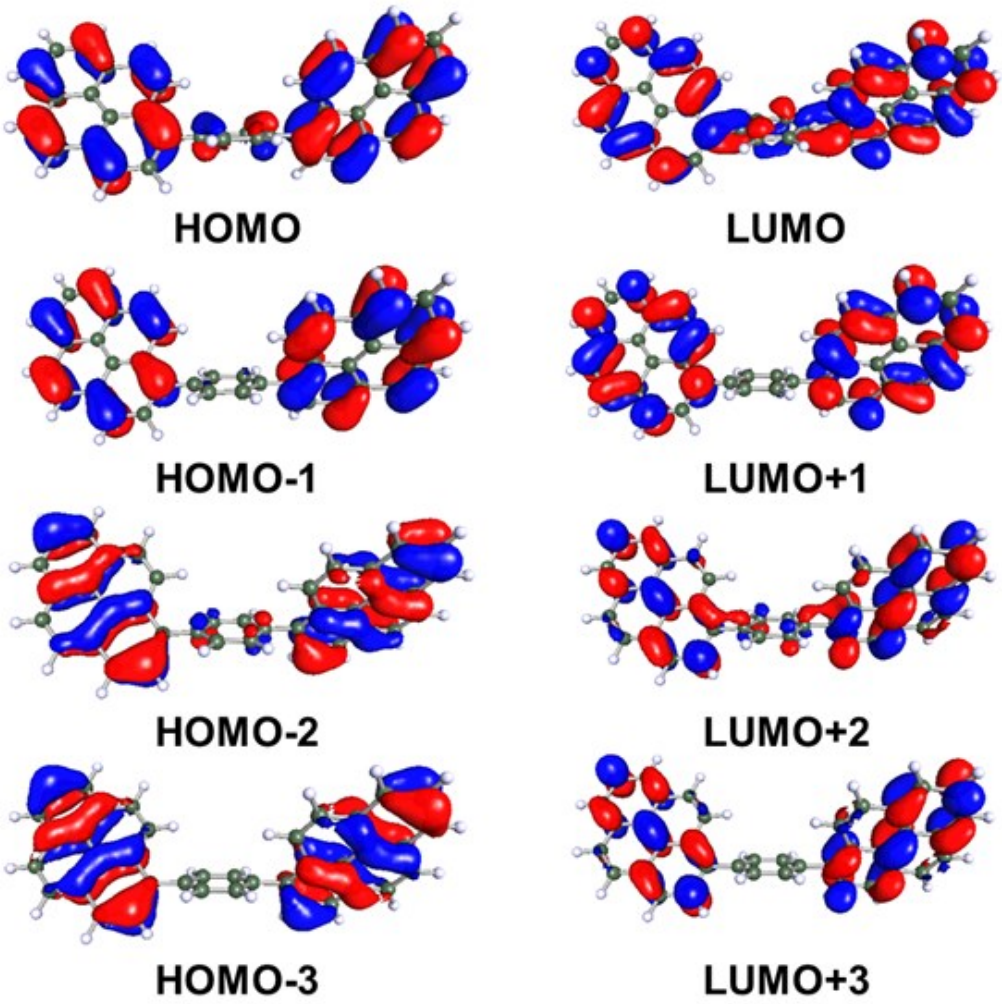

State	S_1	S_2
Transition	HOMO → LUMO+2 (27.3%) HOMO-1 → LUMO+3 (24.1%) HOMO-2 → LUMO (23.1%) HOMO-3 → LUMO+1 (19.7%)	HOMO → LUMO+3 (27.8%) HOMO-1 → LUMO+2 (24.3%) HOMO-3 → LUMO (22.4%) HOMO-2 → LUMO+1 (19.6%)

Figure S9. The molecular orbitals of two transitions ($S_0 \rightarrow S_1$ and $S_0 \rightarrow S_2$) of Py-Benz-Py computed using ADC(2) method and def-TZVP basis set. The contribution is given in parentheses.

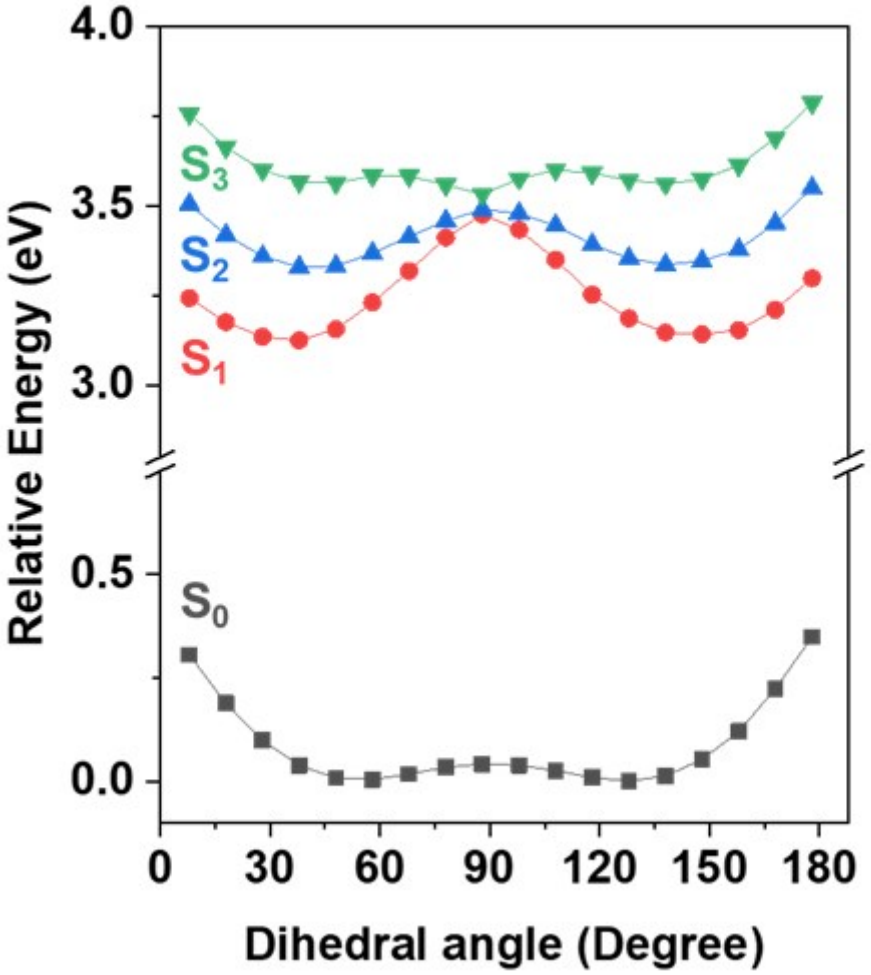

Figure S10. Potential energy surface along the dihedral angle of Py-Benz-Py calculated for the gas phase. All calculations in the ground state were carried out using B3LYP/6-31G* with a relaxed scan. Each point of the excited state was determined by adding the vertical excitation energies to the ground state energy.

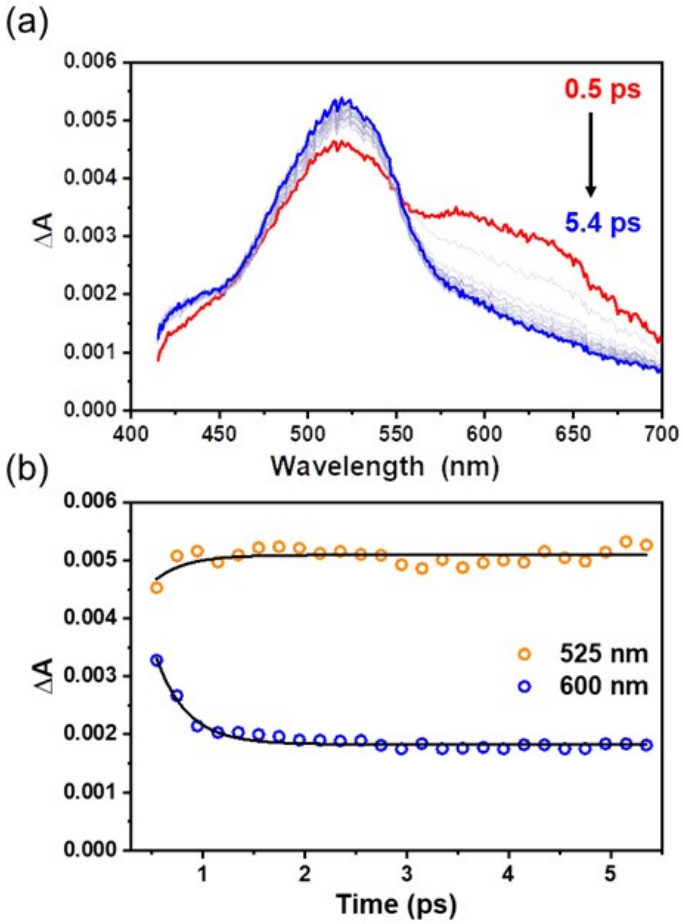

Figure S11. (a) Transient absorption spectra of Py-Benz in DCM. The excitation wavelength is 350 nm. (b) Time profiles monitored at selected wavelengths (orange circle: 525 nm, and blue circle: 600 nm). Fit curves are shown in black solid lines.

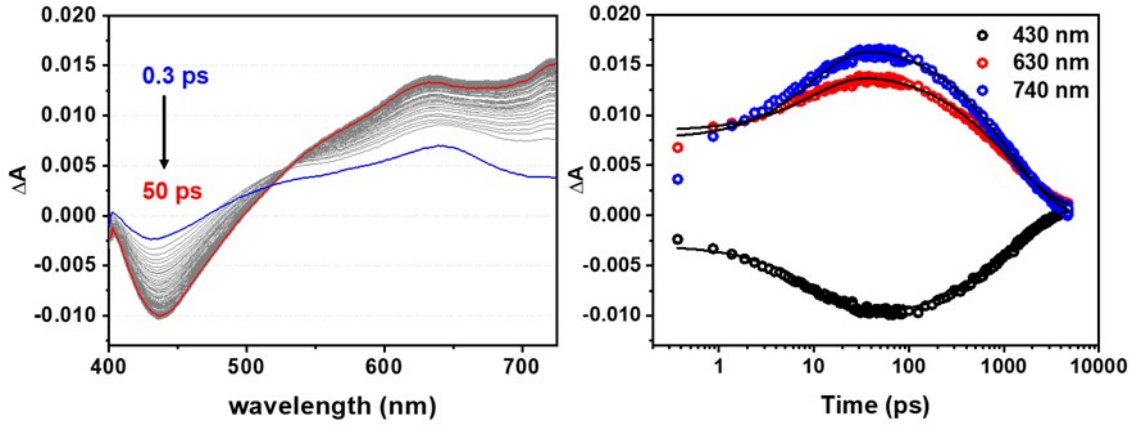

Figure S12. (a) Transient absorption spectra of Py-Benz-Py in CHX. The excitation wavelength is 350 nm. (b) Time profiles monitored at selected wavelengths (black circle: 430 nm, red circle: 630 nm, and blue circle: 740 nm).

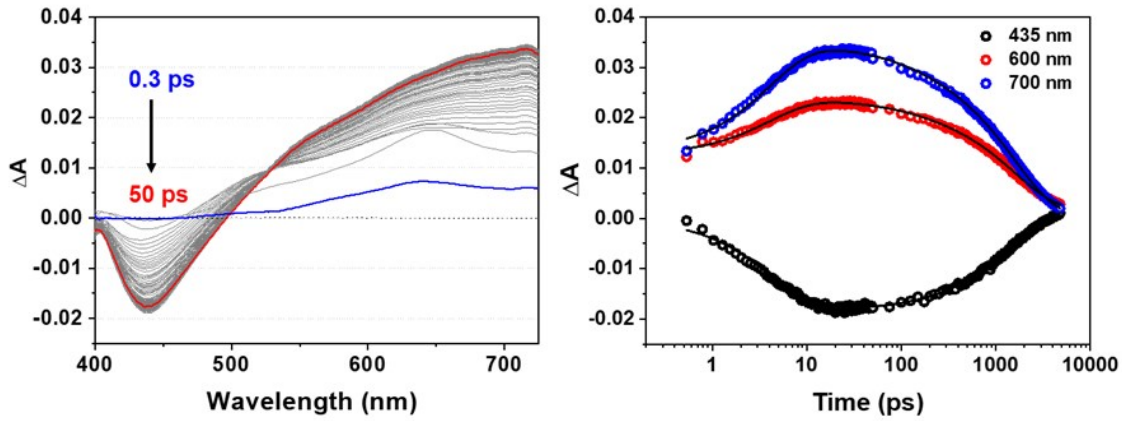

Figure S13. (a) Transient absorption spectra of Py-Benz-Py in EE. The excitation wavelength is 350 nm. (b) Time profiles monitored at selected wavelengths (black circle: 435 nm, red circle: 600 nm, and blue circle: 700 nm). The theoretical fitting curve is shown as a black solid line.

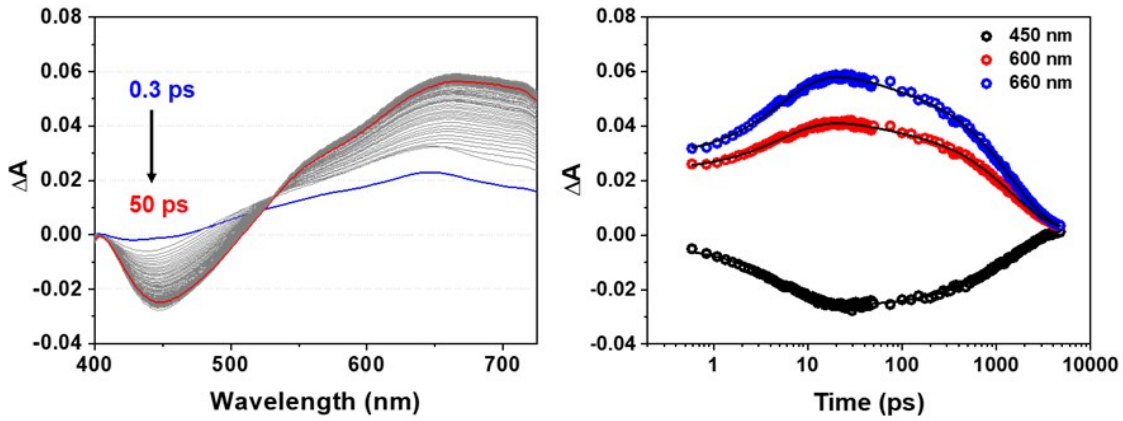

Figure S14. (a) Transient absorption spectra of Py-Benz-Py in THF. The excitation wavelength is 350 nm. (b) Time profiles monitored at selected wavelengths (black circle: 450 nm, red circle: 600 nm, and blue circle: 660 nm). The theoretical fitting curve is shown as a black solid line.

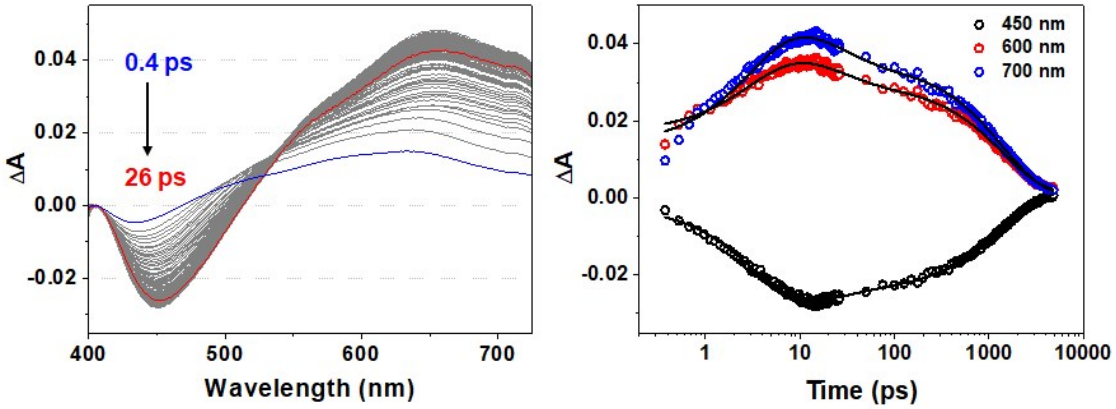

Figure S15. (a) Transient absorption spectra of Py-Benz-Py in DCM. The excitation wavelength is 350 nm. (b) Time profiles monitored at selected wavelengths (black circle: 450 nm, red circle: 600 nm, and blue circle: 700 nm). The theoretical fitting curve is shown as a black solid line.

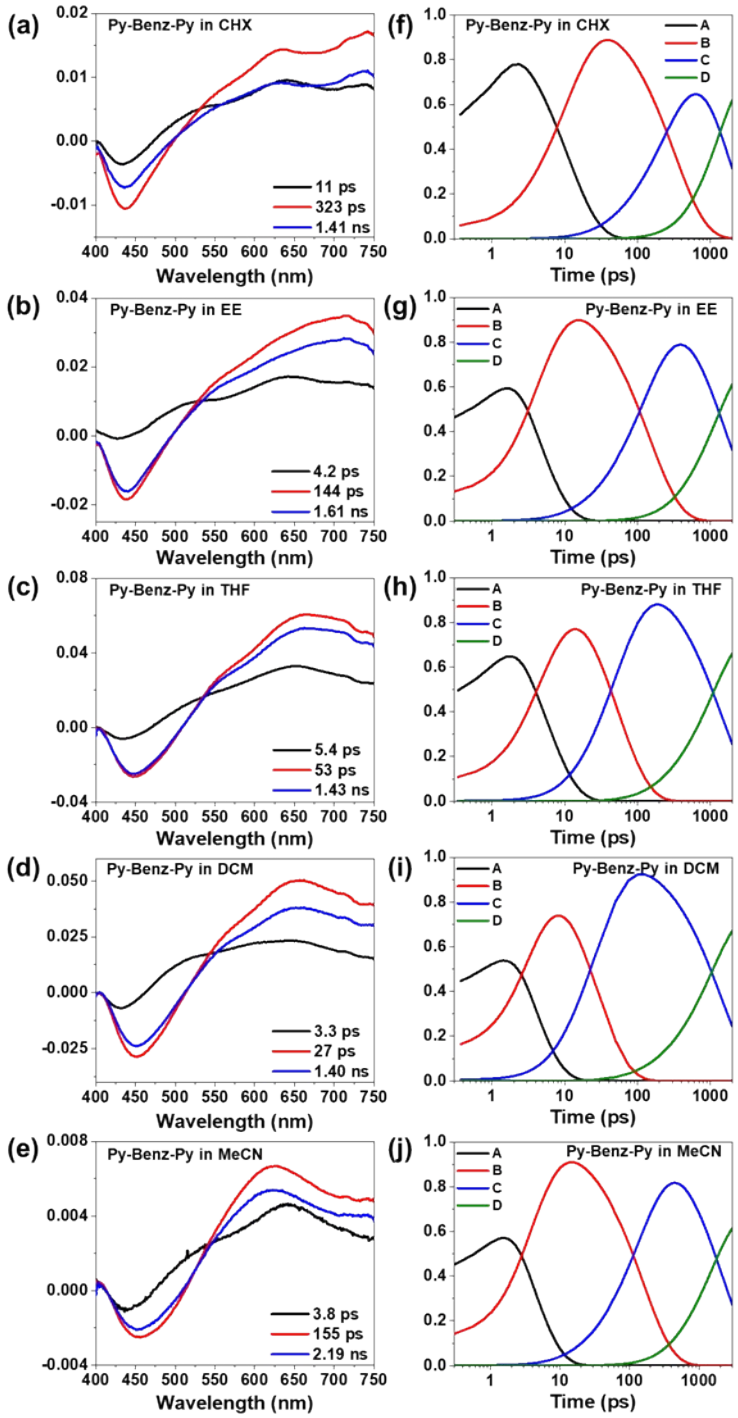

Figure S16. (a-e) The evolution-associated difference spectra (EADS) and (f-j) population changes of Py-Ben-Py in CHX, EE, THF, DCM, and MeCN. A, B, C, and D correspond to the S_1/S_2 mixed state, ICT state, PICT state, and ground state, respectively.

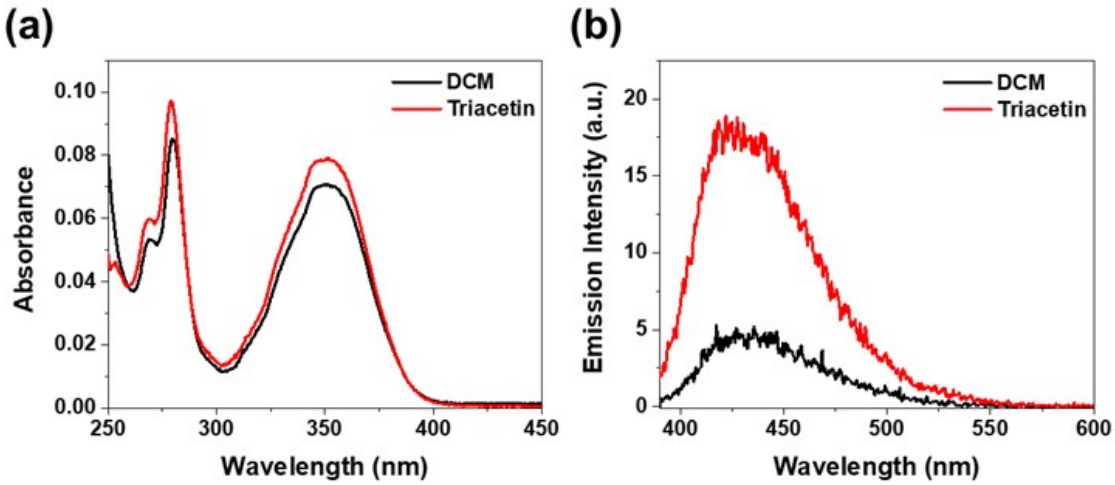

Figure S17. UV-visible absorption (a) and emission spectra of Py-Benz-Py in DCM and triacetin. The viscosities of DCM and triacetin are 0.43 and 23 cP at 20°C, respectively. The excitation wavelength is 380 nm.

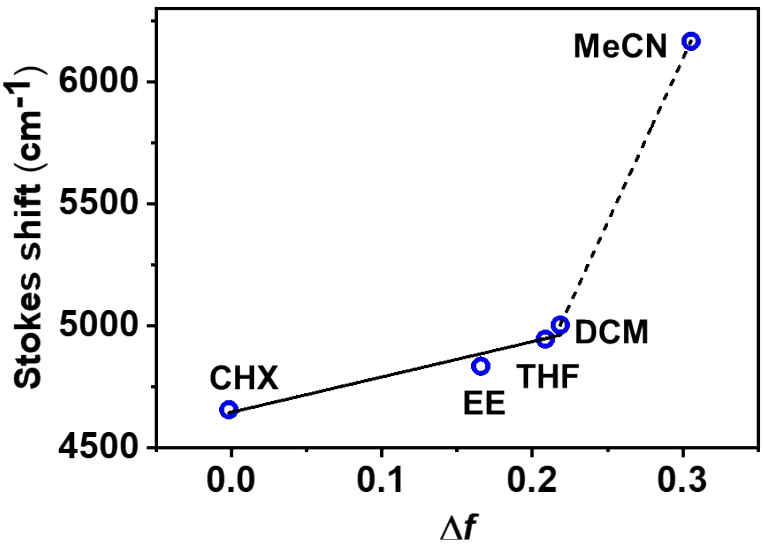

Figure S18. Lippert-Mataga plot for Py-Benz-Py. The Stokes shift of the Py-Benz-Py is plotted against the orientation polarizability (Δf).

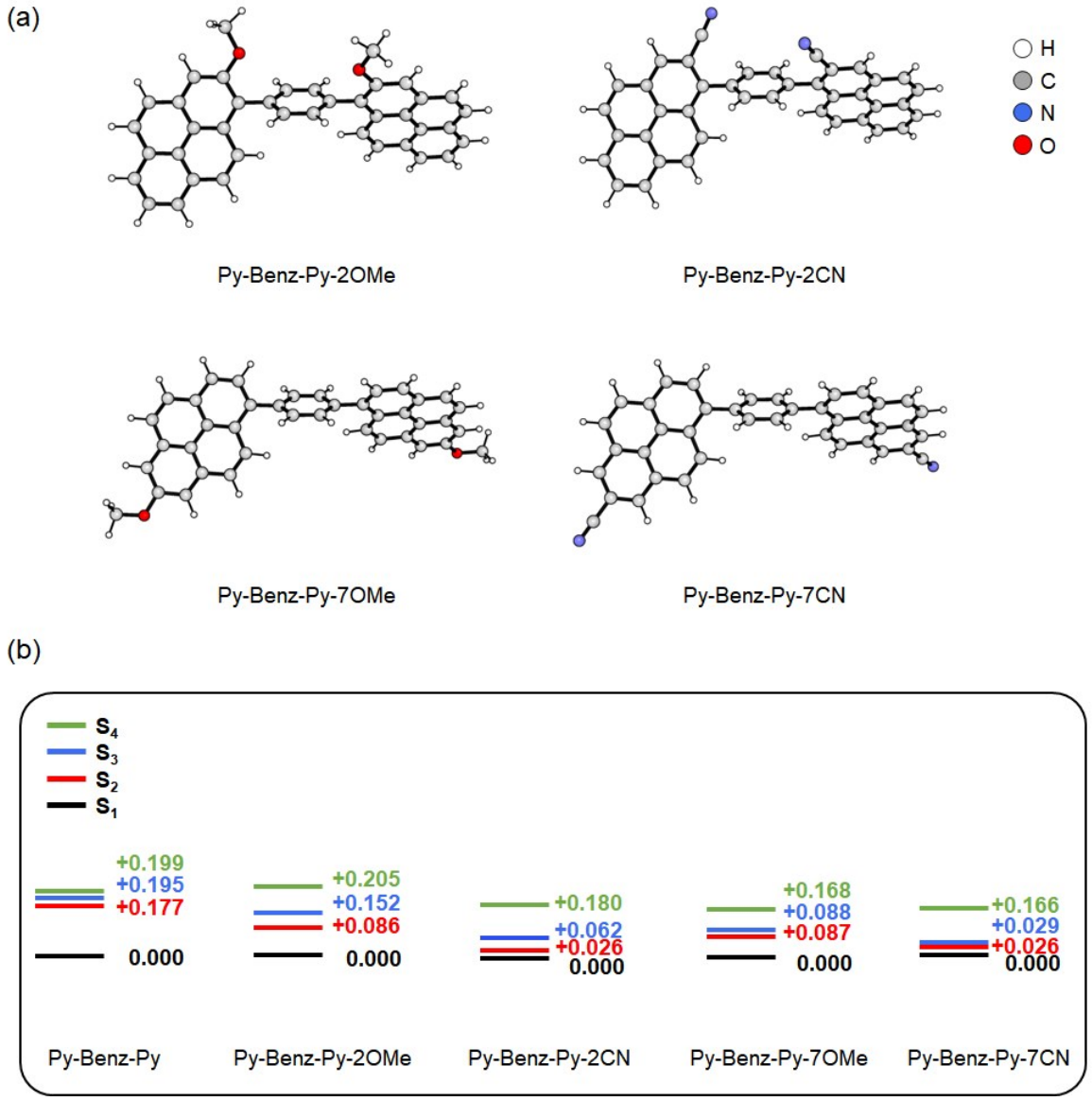

Figure S19. DFT and TDDFT calculated ground state structures and relative energy level diagram for Py-Benz-Py and four substituted Py-Benz-Py compounds. DFT and TDDFT calculations were implemented using CAM-B3LYP/6-31G* and CAM-B3LYP/cc-pVTZ, respectively. (a) DFT optimized structures of four substituted Py-Benz-Py compounds in the ground state. (b) Relative energy levels of transition state compared to each S_1 energy in Py-Benz-Py and all substituted Py-Benz-Py compounds.